Indian Journal of Geo Marine Sciences
Vol.46 (12), December 2017, pp. 2543-2551

# Robust variable-depth path following of an under-actuated autonomous underwater vehicle with uncertainties

Caoyang Yu[1], Xianbo Xiang[1*], Mingjiu Zuo[2] & Guohua Xu[1]

[1]School of Naval Architecture and Ocean Engineering, Huazhong University of Science and Technology, Wuhan 430074, China
[2]College of Information and Electrical Engineering, Naval University of Engineering, Wuhan 430033, China

*[E-mail: xbxiang@hust.edu.cn]

*Received 14 April 2017 ; revised 30 October 2017*

This paper treats the subject of variable-depth path following control of an under-actuated autonomous underwater vehicle (AUV) with multiple uncertainties. The modeling uncertainties of the investigated AUV are composed of inaccurate hydrodynamic coefficients and unknown environmental disturbances. For this uncertain system, a nonlinear control law integrating line-of-sight (LOS) guidance with fuzzy sliding mode control (FSMC) algorithm is designed to guarantee global $\kappa$ -exponentially convergence of path following errors. The LOS guidance in the Serret-Frenet frame is adopted to guide the under-actuated AUV to move towards the curved variable-depth path. The sliding mode control algorithm ensures the stability and the robustness of the designed control law in the presence of multiple uncertainties. The fuzzy logic algorithm is integrated to adjust sliding mode gain in order to weaken chattering. In addition, the angle of attack is considered in the design of dynamics control law to ensure that the under-actuated AUV follows the predefined path with a given resultant speed. Finally, a comparative simulation study illustrates the effectiveness of the designed FSMC algorithm for variable-depth path following of an under-actuated AUV with multiple uncertainties.

**[Keywords:** Path following, Autonomous underwater vehicle (AUV), Under-actuated configuration, Fuzzy sliding mode control (FSMC), Multiple uncertainties]

## Introduction

Over the past two decades, autonomous underwater vehicles (AUVs) have been an important branch of robotics including air, land, surface and underwater vehicles[1,2,3,4,5]. AUVs are playing an important role in marine commercial, scientific and military applications, such as subsea cable tracking and inspection[6,7], three-dimensional seabed reconstruction[8], marine pollution monitoring[9], ocean observation[10], and underwater sampling and monitoring[11]. Yet, the robot control remains a challenging task, primarily due to under-actuated configuration, complicated modeling parameters and unknown environmental disturbances[12,13,14,15,16,17].

For marine robots, motion control scenarios include dynamic positioning[18], path following[19],

* Corresponding author

path tracking[20], and trajectory tracking[21]. Among them, path following is much popular and refers to the case where the control objective is to let marine robot converge to a predefined geometric path without any temporal requirements.

As a matter of fact, various advanced controllers for path following of AUVs have been proposed in recent years. A virtual target for horizontal path following was introduced on the predefined path to avoid the singularity of control algorithm, and then a nonlinear closed loop control law heavily relying on backstepping technique was proposed to steer an under-actuated AUV along the predefined path[22]. This control law was redesigned in horizontal path following control of a fully actuated AUV[23,24]. In order to compensate ocean currents, an indirect disturbance observer was designed, and then a direct adaptive integral line-of-sight (LOS) controller for horizontal path following was proposed to guarantee global convergence of the cross-track error[25]. In addition, proportional–integral–derivative (PID), fuzzy logic and neural network-based controllers have been applied to horizontal plane control[26,27,28,29,30].

Compared with the above horizontal path following, the motion control of AUV in the vertical plane is more difficult since the AUV is subject to added uncertainties resulted by the resorting moment and seawater density change in different depth. A static output feedback controller was designed for vertical path following of an AUV without any uncertainties[31]. A state-dependent Riccati equation method was proposed to obtain a suboptimal control law of depth control for the REMUS AUV with perturbed hydrodynamic parameters[32]. In addition, a self-adaptive fuzzy PID controller was designed for depth attitude control to encounter the uncertainty in parameters[33]. In order to reject ocean wave disturbances, a single input fuzzy logic controller with reduced execution time was proposed for variable-depth tracking control of an underwater vehicle[34]. An adaptive fuzzy logic controller was introduced to solve the depth tracking problem of an AUV in the presence of external disturbances and actuator saturation[35]. Yet, the multiple uncertainties resulted by inaccurate hydrodynamic coefficients and unknown environmental disturbances are not addressed in the above research. In addition, a given surge speed is assumed in the vertical path following control since the under-actuated AUV cannot independently control the heave speed[31-34]. In this case, the resultant speed along the predefined path is unknown in advance.

Motivated by above considerations, this paper addresses the problem of variable-depth path following control for an under-actuated AUV with multiple uncertainties. A nonlinear control law integrating LOS guidance with fuzzy sliding mode control (FSMC) algorithm is designed to guarantee global convergence of path following errors. The sliding mode control (SMC) algorithm ensures the stability and robustness against multiple uncertainties, and the added fuzzy logic algorithm tunes SMC gains to weaken chattering. In addition, the angle of attack is considered in the dynamics control law to ensure that the under-actuated AUV can achieve a given resultant speed rather than a given surge speed.

## Materials and Methods

### *AUV modeling*

The kinematics equations of an AUV in the vertical plane can be described as

$$\begin{cases} \dot{x} = u\cos\theta + w\sin\theta \\ \dot{z} = -u\sin\theta + w\cos\theta \\ \dot{\theta} = q \end{cases} \quad (1)$$

where ( $x$ , $z$ ) defines the inertial position of the AUV, ( $u$ , $w$ ) denotes its linear speed with respect to the inertial frame, $\theta$ is the pitch angle, and $q$ is the pitch angular speed.

Taking into account $U = \sqrt{u^2 + w^2}$ , (1) can be rewritten as

$$\begin{cases} \dot{x} = U\cos\upsilon \\ \dot{z} = -U\sin\upsilon \\ \dot{\upsilon} = q - \dot{\alpha} \end{cases} \quad (2)$$

where $U$ is the resultant speed of AUV, $\upsilon = \theta - \alpha$ is its elevation angle, and $\alpha = \arctan(w/u)$ is its angle of attack.

The dynamics equations of a typical under-actuated AUV in the vertical plane can be described as

$$\begin{cases} m_{11}\dot{u} = -m_{22}wq - \left(d_{11} + d_{u2}|u| + d_{u3}u^2\right)u + \tau_u \\ \qquad + \left(\tau_{Ex}\cos\theta - \tau_{Ez}\sin\theta\right) \\ m_{22}\dot{w} = m_{11}uq - \left(d_{22} + d_{w2}|w| + d_{w3}w^2\right)w \\ \qquad + \left(\tau_{Ex}\sin\theta + \tau_{Ez}\cos\theta\right) \\ m_{33}\dot{q} = \left(m_{22} - m_{11}\right)uw - \left(d_{33} + d_{q2}|q| + d_{q3}q^2\right)q \\ \qquad - B\bar{l}_{cb}\sin\theta + \tau_q + \tau_{Eq} \end{cases} \tag{3}$$

where $m_{(\cdot)}$ are hydrodynamic coefficients, $d_{(\cdot)}$ are hydrodynamic damping coefficients, $B$ is the buoyancy of the AUV, $l_{cb}$ is the metacentric height, $\tau_u$ is the surge control force, and $\tau_q$ is the pitch control torque . In addition, $\tau_{Ex}$ , $\tau_{Ez}$ , and $\tau_{Eq}$ are unknown environmental disturbances in the inertial frame.

In fact, it is difficult for designers to obtain all the accurate hydrodynamic coefficients. We define those modeled dynamics and unmodeled dynamics as $\bar{\cdot}$ and $\Delta(\cdot)$ , namely,

$$\begin{cases} m_{(\cdot)} = \bar{m}_{(\cdot)} + \Delta m_{(\cdot)} \\ d_{(\cdot)} = \bar{d}_{(\cdot)} + \Delta d_{(\cdot)} \\ l_{cb} = \bar{l}_{cb} + \Delta l_{cb} \end{cases} \tag{4}$$

Then (3) can be rewritten as

$$\begin{cases} \bar{m}_{11}\dot{u} = -\bar{m}_{22}wq - \left(\bar{d}_{11} + \bar{d}_{u2}|u| + \bar{d}_{u3}u^2\right)u + \tau_u + \varepsilon_u \\ \bar{m}_{22}\dot{w} = \bar{m}_{11}uq - \left(\bar{d}_{22} + \bar{d}_{w2}|w| + \bar{d}_{w3}w^2\right)w + \varepsilon_w \\ \bar{m}_{33}\dot{q} = \left(\bar{m}_{22} - \bar{m}_{11}\right)uw - \left(\bar{d}_{33} + \bar{d}_{q2}|q| + \bar{d}_{q3}q^2\right)q \\ \qquad - Bl_{cb}\sin\theta + \tau_q + \varepsilon_q \end{cases} \tag{5}$$

with

$$\begin{cases} \varepsilon_u = -\Delta m_{22}wq + \left(\Delta d_{11} + \Delta d_{u2}|u| + \Delta d_{u3}u^2\right)u \\ \qquad - \Delta m_{11}\dot{u} + \left(\tau_{Ex}\cos\theta - \tau_{Ez}\sin\theta\right) \\ \varepsilon_w = \Delta m_{11}uq - \left(\Delta d_{22} + \Delta d_{w2}|w| + \Delta d_{w3}w^2\right)w \\ \qquad - \Delta m_{22}\dot{w} + \left(\tau_{Ex}\sin\theta + \tau_{Ez}\cos\theta\right) \\ \varepsilon_q = \left(\Delta m_{22} - \Delta m_{11}\right)uw - \Delta m_{33}\dot{q} - B\Delta l_{cb}\sin\theta \\ \qquad - \left(\Delta d_{33} + \Delta d_{q2}|q| + \Delta d_{q3}q^2\right)q + \tau_{Eq} \end{cases} \tag{6}$$

**Assumption 1**. For unmodeled dynamics (6) in system (5), there exist positive constants $\bar{\varepsilon}_u$ , $\bar{\varepsilon}_w$ , and $\bar{\varepsilon}_q$ , such that $\varepsilon_u$ , $\varepsilon_w$ , and $\varepsilon_q$ satisfy the relationships $|\varepsilon_u| \le \bar{\varepsilon}_u$ , $|\varepsilon_w| \le \bar{\varepsilon}_w$ , and $|\varepsilon_q| \le \bar{\varepsilon}_q$ [36].

*Problem statement*

As depicted in Figure 1, $P$ is a virtual target point on the predefined path $\boldsymbol{P}_P(s)$. Similarly to the AUV, let the position and elevation angle of point $P$ be denoted by ($x_F$, $y_F$, $\upsilon_F$). Associated with $P$, the Serret–Frenet frame $\{F\}$ can be built by using the elevation angle orientation of $P$ as its $x$-axis. In addition, $Q$ is the center of mass of AUV which is required to converge to and follow the predefined path $\boldsymbol{P}_P(s)$. $x_e$ and $z_e$ are the position errors between the AUV and point $P$ in the frame $\{F\}$.

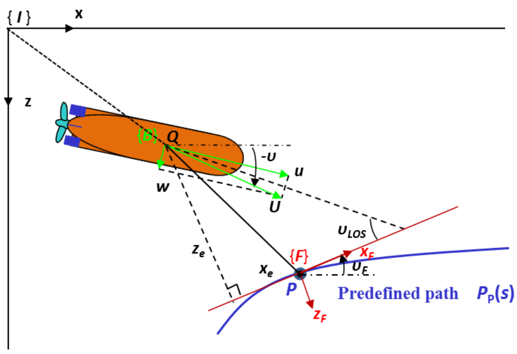


Fig.1-LOS guidance and frame definitions of path following

The problem of robust variable-depth path following control for an under-actuated AUV can be formulated as

$$\lim_{t\to\infty}\left(s_e, \upsilon_e, U_e\right) = \mathbf{0} \tag{7}$$

with

$$\begin{cases} s_e = \sqrt{x_e^2 + z_e^2} \\ \upsilon_e = \upsilon - \upsilon_F \\ U_e = U - U_d \end{cases} \tag{8}$$

where $U_d$ is the given resultant speed. Note that the first term in (7) demands that the center of mass of AUV converge to the path in the presence of multiple uncertainties; the second term demands that the resultant speed of the AUV align with the tangent of the predefined path; and the third term demands that the resultant speed of the AUV achieve a desired profile.

*Kinematics controller*

According to Figure 1, the path following error ($x_e$, $y_e$, $\upsilon_e$) built in the frame {$F$} can be written as

$$\begin{cases} x_e = (x - x_F)\cos\upsilon_F - (z - z_F)\sin\upsilon_F \\ z_e = (x - x_F)\sin\upsilon_F + (z - z_F)\cos\upsilon_F \\ \upsilon_e = \upsilon - \upsilon_F \end{cases} \quad (9)$$

By combining (2) and $\dot{\upsilon}_F = \kappa U_F$, differentiating (9) yields that

$$\begin{cases} \dot{x}_e = -U_F(1 + \kappa z_e) + U\cos\upsilon_e \\ \dot{z}_e = \kappa U_F x_e - U\sin\upsilon_e \\ \dot{\upsilon}_e = q - \dot{\alpha} - \kappa U_F \end{cases} \quad (10)$$

where the curvature of the predefined path is $\kappa = (x'_F z''_F - x''_F z'_F) / ({x'_F}^2 + {z'_F}^2)^{3/2}$ with $x'_F = \partial x_F / \partial\varpi$, $x''_F = \partial^2 x_F / \partial\varpi^2$, $z'_F = \partial z_F / \partial\varpi$ and $z''_F = \partial^2 z_F / \partial\varpi^2$, and $U_F = \dot{s}\sqrt{{x'_F}^2 + {z'_F}^2}$ is the resultant speed of point $P$ on the predefined path.

Similarly to [22,23,24], the following vertical –plane LOS guidance angle is introduced to guide the under-actuated AUV to adjust elevation angle and converge to the predefined depth path

$$\upsilon_{LOS} = \arctan(z_e/\Delta z) \quad (11)$$

where $\Delta z$ is a positive constant.

As the primary control objective of vertical variable-depth path following control is to drive the position and orientation errors ($s_e$, $\upsilon_e$) to zero, we first define the following positive definite Lyapunov function candidate

$$V_1 = \frac{1}{2}\left[s_e^2 + (\upsilon_e - \upsilon_{LOS})^2\right] \quad (12)$$

Resorting to (10), the derivative of $V_1$ can be calculated as

$$\begin{aligned} \dot{V}_1 = &-x_e U_F + U x_e\cos\upsilon_e - U z_e\sin\upsilon_e \\ &+ (\upsilon_e - \upsilon_{LOS})(\dot{\upsilon}_e - \dot{\upsilon}_{LOS}) \end{aligned} \quad (13)$$

It is natural for us to choose the kinematics control laws of variable-depth path following as

$$\begin{cases} U_F = k_1 x_e + U\cos\upsilon_e \\ \dot{\upsilon}_e = \dot{\upsilon}_{LOS} + z_e U \dfrac{\sin\upsilon_e - \sin\upsilon_{LOS}}{\upsilon_e - \upsilon_{LOS}} \\ \qquad - k_2(\upsilon_e - \upsilon_{LOS}) \end{cases} \quad (14)$$

where $k_1$ and $k_2$ are positive constants. Note that the first equation in (14) defines the desired resultant speed of point $P$ on the path, and the second equation is designed for the pitch motion of AUV.

Substituting (14) into (13) , it has

$$\dot{V}_1 = -k_1 x_e^2 - \frac{U z_e^2}{\sqrt{z_e^2 + \Delta_z^2}} - k_2(\upsilon_e - \upsilon_{LOS})^2 \quad (15)$$

which means that $\dot{V}_1$ is negative definite. According to Lyapunov's second method for stability, it is concluded that

$$\lim_{t\to\infty}(x_e, z_e, \upsilon_e - \upsilon_{LOS}) = \mathbf{0} \quad (16)$$

Recalling $U_F = \dot{s}\sqrt{{x'_F}^2 + {z'_F}^2}$ in (14) yields the virtual control law of point $P$ on the path as

$$\dot{s} = (k_1 x_e + U\cos\upsilon_e) / \sqrt{{x'_F}^2 + {z'_F}^2} \quad (17)$$

**Remark 1.** Note that the above virtual control law of point $P$ on the predefined path can be regarded as an extra degree of freedom for variable-depth path following and can be easily guaranteed. However, the point motion on the trajectory is time-dependent and cannot be adaptively adjusted in trajectory tracking.

*Dynamics controller*

By combining the third equation in (10) with the second equation in (14), the desired pitch angular speed $q_d$ of AUV can be defined as

$$\begin{aligned} q_d = &\dot{\upsilon}_{LOS} + z_e U \frac{\sin\upsilon_e - \sin\upsilon_{LOS}}{\upsilon_e - \upsilon_{LOS}} - k_2(\upsilon_e - \upsilon_{LOS}) \\ &+ \dot{\alpha} + \kappa U_F \end{aligned} \quad (18)$$

Though the kinematics design based on the LOS guidance law, the control objective in the dynamics stage for variable-depth path following of an under-actuated AUV becomes tracking the desired resultant speed and pitch angular speed. Hence, we consider the following positive definite Lyapunov function candidate for the whole system

$$V_2 = V_1 + \frac{1}{2}\left({U_e}^2 + {q_e}^2\right) \quad (19)$$

with $q_e = q - q_d$.

It is well known that $u = U\cos\alpha$. For an under-actuated AUV with a given resultant speed, the desired surge speed $u_d$ can be designed as

$$u_d = U_d \cos\alpha \tag{20}$$

Substituting $u = U\cos\alpha$ and (20) into (19), $V_2$ can be rewritten as

$$V_2 = V_1 + \frac{1}{2}\left(\frac{1}{\cos^2\alpha}u_e^2 + q_e^2\right) \tag{21}$$

with $u_e = u - u_d$.

The derivative of $V_2$ is

$$\begin{aligned}\dot{V}_2 &= -k_1 x_e^2 + \frac{1}{\cos^2\alpha}u_e\dot{u}_e + \frac{\tan\alpha}{\cos^2\alpha}u_e^2 \\ &+ (\upsilon_e - \upsilon_{LOS})(\dot{\upsilon}_e - \dot{\upsilon}_{LOS}) - Uz_e\sin\upsilon_e + q_e\dot{q}_e\end{aligned} \tag{22}$$

It is natural for us to choose the speed dynamics of variable-depth path following as

$$\begin{cases}\dot{u} = \dot{u}_d - (k_3 + \dot{\alpha}\tan\alpha)u_e \\ \dot{q} = \dot{q}_d - (\upsilon_e - \upsilon_{LOS}) - k_4 q_e\end{cases} \tag{23}$$

where $k_3$ and $k_4$ are positive constants.

As SMC is a robust approach to control a nonlinear system with internal and external uncertainties[2,12,14], we resort to the SMC algorithm and design the following dynamics control laws

$$\begin{cases}\tau_u = \bar{m}_{22}wq + \left(\bar{d}_{11} + \bar{d}_{u2}|u| + \bar{d}_{u3}u^2\right)u \\ \quad + \bar{m}_{11}\left[\dot{u}_d - (k_3 + \dot{\alpha}\tan\alpha)u_e - \kappa_u \operatorname{sgn} u_e\right] \\ \tau_q = -(\bar{m}_{22} - \bar{m}_{11})uw + B\bar{l}_{cb}\sin\theta \\ \quad + \left(\bar{d}_{33} + \bar{d}_{q2}|q| + \bar{d}_{q3}q^2\right)q \\ \quad + \bar{m}_{33}\left[\dot{q}_d - k_4 q_e - (\upsilon_e - \upsilon_{LOS}) - \kappa_q \operatorname{sgn} q_e\right]\end{cases} \tag{24}$$

Substituting (24) into (5), it has

$$\begin{cases}\dot{u} = \dot{u}_d - (k_3 + \dot{\alpha}\tan\alpha)u_e - \kappa_u \operatorname{sgn} u_e + \varepsilon_u \\ \dot{q} = \dot{q}_d - (\upsilon_e - \upsilon_{LOS}) - k_4 q_e - \kappa_q \operatorname{sgn} q_e + \varepsilon_q\end{cases} \tag{25}$$

Hence, the derivative of $V_2$ under the dynamics control laws (24) is

$$\begin{aligned}\dot{V}_2 &= -k_1 x_e^2 - \frac{Uz_e^2}{\sqrt{z_e^2 + \Delta_z^2}} - k_2(\upsilon_e - \upsilon_{LOS})^2 - k_3 U_e^2 \\ &- k_4 q_e^2 - \frac{1}{\cos^2\alpha}\left(\kappa_u|u_e| - \varepsilon_u u_e\right) - \left(\kappa_q|q_e| - \varepsilon_q q_e\right)\end{aligned} \tag{26}$$

which means that $\dot{V}_2$ is negative definite if $\kappa_u \ge \bar{\varepsilon}_u$ and $\kappa_q \ge \bar{\varepsilon}_q$. According to Lyapunov's second method for stability, it is concluded that

$$\lim_{t\to\infty}(s_e, \upsilon_e - \upsilon_{LOS}, U_e, q_e) = \mathbf{0} \tag{27}$$

**Assumption 2**. In this paper, $z_e$ is assumed to be bounded and $U$ keeps positive[23,36].

Based on Assumption 2, there exists a positive number $k_s = \min\left\{k_1, U\big/\sqrt{z_e^2 + \Delta_z^2}\right\}$. Subsequently, we can choose $k = \min\{k_s, k_2, k_3, k_4\}$ in order to rewritten the derivative of $V_2$ as

$$\begin{aligned}\dot{V}_2 &\le -k_s s_e^2 - k_2(\upsilon_e - \upsilon_{LOS})^2 - k_3 U_e^2 - k_4 q_e^2 \\ &\le -2kV_2\end{aligned} \tag{28}$$

Hence, the equilibrium point in (21) is uniformly globally asymptotically and locally exponentially stable. According to [37], the equilibrium point of the whole system is globally $\kappa$-exponentially stable.

**Remark 2**. By recalling $\upsilon_{LOS} = \arctan(z_e/\Delta z)$, it can be concluded that $\lim_{t\to\infty} z_e = 0$ is equivalent to $\lim_{t\to\infty}\upsilon_{LOS} = 0$. Hence, (27) also means $\lim_{t\to\infty}\upsilon_e = 0$, which indicates that all the control objectives in variable-depth path following can be achieved under the control laws (24).

In order to guarantee the absolute stability of the above system, $\kappa_u$ and $\kappa_q$ should be chosen very large to ensure $\kappa_u \ge \bar{\varepsilon}_u$ and $\kappa_q \ge \bar{\varepsilon}_q$. However, as the gains become large, the controller will suffer from the obvious chattering. It is well known that fuzzy logic algorithm can provide a formal methodology to represent expert knowledge on how to control a nonlinear uncertain system[33,34,38,39,40,41]. Hence, fuzzy logic is adopted in this paper to adaptively tune the SMC gains in order to reduce chattering. When the errors meet the condition of the SMC law, namely $u_e\dot{u}_e, q_e\dot{q}_e < 0$, the SMC gains $\Delta\kappa_u(u_e\dot{u}_e)$, $\Delta\kappa_q(q_e\dot{q}_e)$ will decrease to reduce chattering; While the errors do not meet the condition of the SMC law, namely $u_e\dot{u}_e, q_e\dot{q}_e > 0$, the above SMC gains will increase to ensure error convergence, which can be formulated as

$$\begin{cases}\kappa_u = \kappa_{u0} + \int_0^t \Delta\kappa_u(u_e\dot{u}_e)\,dt \\ \kappa_q = \kappa_{q0} + \int_0^t \Delta\kappa_q(q_e\dot{q}_e)\,dt\end{cases} \tag{29}$$

The structure of fuzzy logic controller is depicted in Figure 2, where the input is $u_e\dot{u}_e$ or $q_e\dot{q}_e$, and the output is $\Delta\kappa_u$ or $\Delta\kappa_q$. The fuzzy logic implementation includes fuzzification, fuzzy inference and defuzzification.

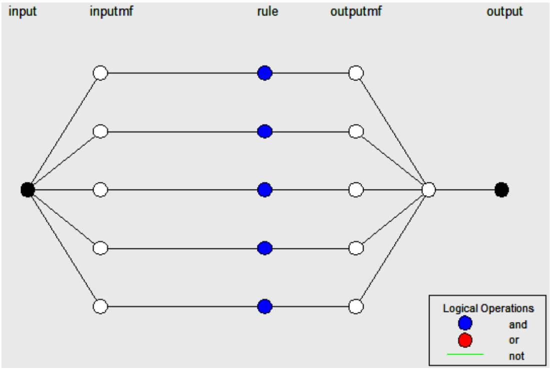


Fig.2-The structure of fuzzy logic controller

Taking the surge control for example, the membership functions (MF) of the input and the output are Gaussian function in Figure 3 and singleton in Table 1, respectively. Both of them have five types of fuzzy subsets, namely PB, PM, ZO, NM, and NB, representing positive large, positive medium, zero, negative medium, and negative large, respectively.

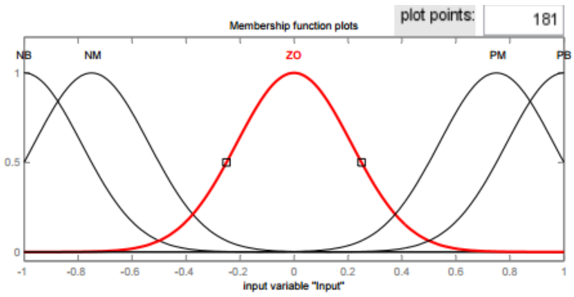


Fig.3-The membership function of fuzzy input variable

Table-1 Fuzzy output singleton

| MF | NB | NM | ZO | PM | PB |
|---|---|---|---|---|---|
| Value | -1 | -0.5 | 0 | 0.5 | 1 |

The fuzzy rules of SMC gains are designed as

Table-2 Fuzzy rules

R1: IF $u_e\dot{u}_e$ is PB THEN $\Delta\kappa_u$ is PB

R2: IF $u_e\dot{u}_e$ is PM THEN $\Delta\kappa_u$ is PM

R3: IF $u_e\dot{u}_e$ is ZO THEN $\Delta\kappa_u$ is ZO

R4: IF $u_e\dot{u}_e$ is NM THEN $\Delta\kappa_u$ is NM

R5: IF $u_e\dot{u}_e$ is NB THEN $\Delta\kappa_u$ is NB

The output of the fuzzy controller can be calculated by adopting the center of area method and is shown in Figure 4. In this paper, the gain tuning method of pitch control is the same as that of surge control and is omitted.

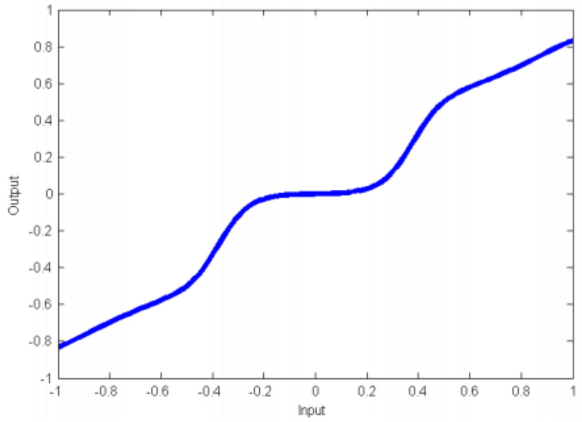


Fig.4-The output of fuzzy logic controller

## Results and Discussion

In order to illustrate the performance of the designed FSMC-based path following controller, a comparative numerical study is carried out by using an AUV, whose accurate hydrodynamic coefficients and modeled coefficients in the simulation are listed in Table 3.

Table-3 AUV hydrodynamic coefficients

| | |
|---|---|
| $m_{11}$=1116kg | $m_{22}$=2133kg |
| $m_{33}$=4061kgm$^2$ | $d_{11}$=25.5kgs$^{-1}$ |
| $d_{22}$=138kgs$^{-1}$ | $d_{33}$=490kgm$^2$s$^{-1}$ |
| $d_{u2}$=0 | $d_{u3}$=0 |
| $d_{w2}$=920.1kgm$^{-2}$s | $d_{q2}$=0 |
| $d_{w3}$=750kgm$^{-3}$s$^2$ | $d_{q3}$=0 |
| $B$=10690.9N | $l_{cb}$=0.0065m |
| $\bar{m}_{11}$ =892.8kg | $\bar{m}_{22}$ =1706.4kg |
| $\bar{m}_{33}$ =3654.9kgm$^2$ | $\bar{d}_{33}$ =340kgm$^2$s$^{-1}$ |
| $\bar{d}_{11}$ =22.95kgs$^{-1}$ | $\bar{l}_{cb}$ =0.00455m |

In this numerical study, the AUV is required to follow a variable-depth path parameterized as

$$\begin{cases} x_F = s \\ z_F = 10\left[1+0.25\tanh\left(\dfrac{s-75}{15}\right)\right] \end{cases} \quad (30)$$

The unknown environmental disturbances in the inertial frame are

$$\begin{cases} \tau_{Ex} = -223.2 f(t) \\ \tau_{Ez} = 213.3 f(t) \\ \tau_{Eq} = -406.1 f(t) \end{cases} \quad (31)$$

with $f(t) = 1 + 0.1\sin(2t)$ .

The initial conditions of AUV are $x = 2$ m, $z = 11$ m, $\theta = 0$ rad, $u = 1.5$ m/s, $w = 0$ m/s, and $q = 0$ rad/s . The given resultant speed is $U_d = 2$ m/s . The spatial convergence of variable-depth path following under the SMC law and the proposed FSMC law is described in Figure 5, where the under-actuated AUV first surfaces up the plane of 7.5 m depth and then dives to the plane of 12.5 m depth. Although the AUV converges to this predefined path, their performance is different from each other.

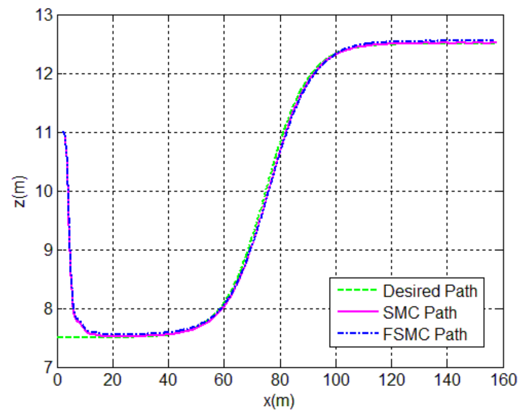


Fig.5-Spatial convergence of variable-depth path following

As shown in Figure 6, the path following errors including the speed error, orientation error and position error, finally reduce to zero. Hence, all the control objectives have been achieved. Figure 7 gives the transitions of the linear and angular speeds of the AUV in the variable-depth path following control. Through the comparison between those two figures, it is obvious that the error and the speed chatter slightly under the SMC law, especially the speed error, the surge speed, and the pitch angular speed. However, the FSMC law shows better path following performance against multiple uncertainties resulted by inaccurate hydrodynamic coefficients and environmental disturbances.

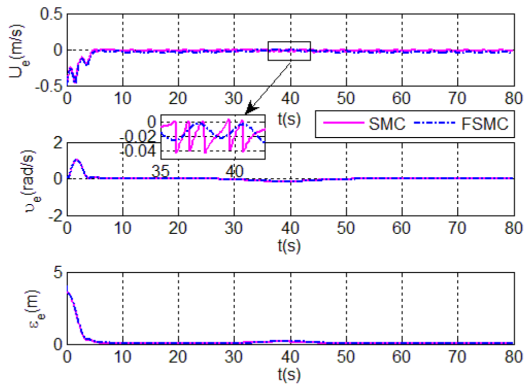


Fig.6-Control errors of variable-depth path following

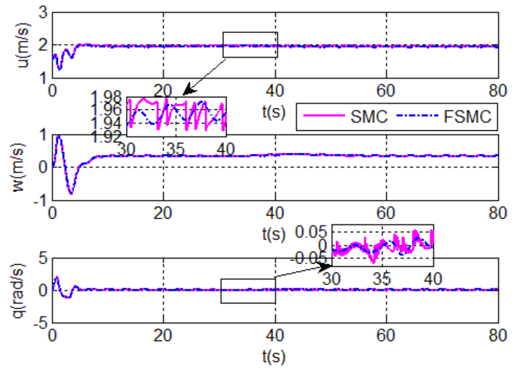


Fig.7-The linear and angular speeds of AUV

In addition, it can be found that the heave speed of the under-actuated AUV is not zero form Figure 7. As depicted in Figure 8, the angle of attack is not zero and its derivative is time-varying. Hence, the angle of attack cannot be neglected and the consideration in the dynamics control law is necessary.

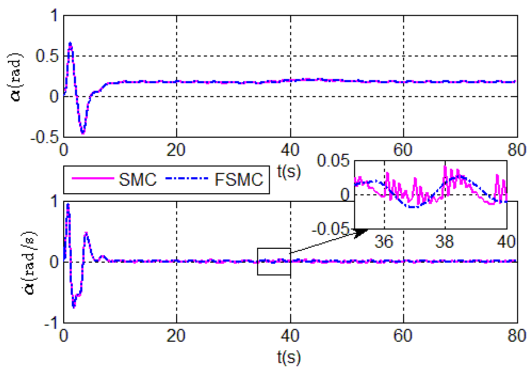


Fig.8-Angle of attack and its derivative

As shown in Figure 9, the control inputs of the SMC law chatter while those of FSMC law are relatively smooth. Hence, the added fuzzy logic is beneficial for weakening chattering of the control inputs and saving energy.

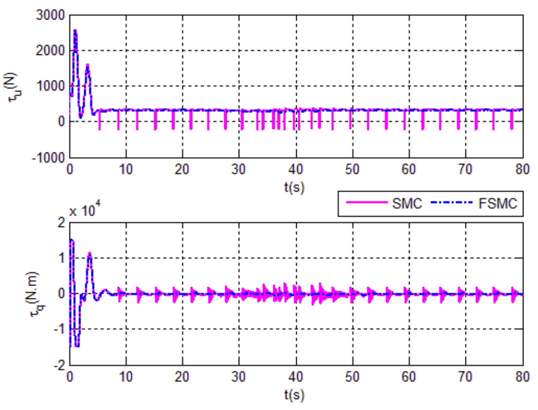


Fig.9-AUV control inputs

## Conclusions

This paper proposes a nonlinear control law integrating LOS guidance with FSMC algorithm, in order to guarantee global $\kappa$ -exponentially convergence of variable-depth path following of an under-actuated AUV with multiple uncertainties. The fuzzy logic algorithm in this FSMC system can weaken chattering. In addition, the angle of attack is considered to ensure that the under-actuated AUV can achieve a given resultant speed. Finally, a comparative numerical study shows that the FSMC law performs better than the classical SMC law.

## Acknowledgment

This work is supported by National Natural Science Foundation of China (under Grant 51579111 and 51209100), the Fundamental Research Funds for the Central Universities (under Grant 2017KFYXJJ005), State Key Laboratory of Ocean Engineering (under Grant 1504), and International Exchanges of the UK Royal Society (under Grant IE161588).

## References

1 Bogue, R., Underwater robots: A review of technologies and applications, *Ind. Robot*, 42(2015) 186-191.
2 Xiang, X.B, Liu, C., Su, H.S. & Zhang, Q., On decentralized adaptive full-order sliding mode control of multiple UAVs, *ISA Trans.* (in press), 2017, DOI: 10.1016/j.isatra.2017.09.008.
3 Zhang, Q., Lapierre, L. & Xiang, X.B., Distributed control of coordinated path tracking for networked nonholonomic mobile vehicles, *IEEE Trans. Ind. Inform.*, 9(2013) 472-484.
4 Yang, S.L., Han, Z.T., Pan, X.X., Yan, Z.J. & Yu, J.Q., Nitrogen oxide removal using seawater electrolysis in an undivided cell for ocean-going vessels, *RSC Adv.*, 6(2016) 114623-114631.
5 Isa, K. & Arshad, M.R., Modeling and motion control of a hybrid-driven underwater glider, *Indian J. Mar. Sci.*, 42(2013) 971-979.
6 Xiang, X.B., Yu, C.Y., Niu, Z.M. & Zhang, Q., Subsea cable tracking by autonomous underwater vehicle with magnetic sensing guidance, *Sensors*, 16(2016) 1335.
7 Yu, C.Y., Xiang, X.B., Lapierre, L. & Zhang, Q., Robust magnetic tracking of subsea cable by AUV in the presence of sensor noise and ocean currents, *IEEE J. Oceanic Eng.* (in press), 2017, DOI: 10.1109/JOE.2017.2768105.
8 Zhang, L., Jouvencel, B., Fang, Z. & Xiang, X.B., 3D reconstruction of seabed surface through sonar data of AUVs, *Indian J. Mar. Sci.*, 41(2012) 509-515.
9 Tonacci, A., Lacava, G., Lippa, M.A., Lupi, L., Cocco, M. & Domenici, C., Electronic nose and AUV: A novel perspective in marine pollution monitoring, *Mar. Technol. Soc. J.*, 49(2015) 18-24.
10 Kadir, H.A. & Arshad, M.R., Ocean observation system using multi blimp system with animal inspired consensus decision making, *Indian J. Mar. Sci.*, 44(2015) 1951-1961.
11 Xiang, X.B., Yu, C.Y., Zheng, J.R. & Xu, G.H., Motion forecast of intelligent underwater sampling apparatus - Part I: Design and algorithm, *Indian J. Mar. Sci.*, 44(2015) 1962-1970.
12 Cui, R.X., Chen, L.P., Yang, C.G. & Chen, M., Extended state observer-based integral sliding mode control for an underwater robot with unknown disturbances and uncertain nonlinearities, *IEEE Trans. Ind. Electron.*, 64(2017) 6785-6795.
13 Xiang, X.B., Yu, C.Y. & Zhang, Q., Robust fuzzy 3D path following for autonomous underwater vehicle subject to uncertainties, *Comput. Oper. Res.*, 84(2017) 165-177.
14 Chu, Z.Z., Xiang, X.B., Zhu, D.Q., Luo, C.M. & Xie, D., Adaptive fuzzy sliding mode diving control for autonomous underwater vehicle with input constraint, *Int. J. Fuzzy Syst.* (in press), 2017, DOI: 10.1007/s40815-017-0390-2.
15 Wang, N., Sun, J.C., Han, M., Zheng, Z.J. & Er, M.J., Adaptive approximation-based regulation control for a class of uncertain nonlinear systems without feedback linearizability, *IEEE Trans. Neural Newt. Learn. Syst.*, (in press), 2017, DOI: 10.1109/TNNLS.2017.2738918.
16 Zhang, Q., Liu, R.F., Chen, W.B. & Xiong, C.H., Simultaneous and continuous estimation of shoulder and elbow kinematics from surface EMG signals, *Front. Neurosci.*, 11(2017), DOI: 10.3389/ins.2017.00280.
17 Kang, H.S., Kim, M.H., Bhat Aramanadka, S.S., Kang, H.Y. & Lee, K.Q., Suppression of tension variations in hydro-pneumatic riser tensioner by using force compensation control, *Ocean Syst. Eng.*, 7(2017) 225-246.
18 Gao, J., Wu, P.G., Li, T.R. & Proctor, A., Optimization-based model reference adaptive control for dynamic positioning of a fully actuated underwater

vehicle, *Nonlinear Dyn.*, 87(2017) 2611-2623.
19 Yi, B.W., Qiao, L. & Zhang, W.D., Two-time scale path following of underactuated marine surface vessels: Design and stability analysis using singular perturbation methods, *Ocean Eng.*, 124(2016) 287-297.
20 Do, K.D., Path-tracking control of underactuated ships under tracking error constraints, *J. Marine Sci. Appl.*, 14(2015) 343-354.
21 Zheng, Z.W., Jin, C., Zhu, M. & Sun, K.M., Trajectory tracking control for a marine surface vessel with asymmetric saturation actuators, *Robot. Auton. Syst.*, 97(2017) 83–91.
22 Lapierre, L. & Soetanto, D., Nonlinear path-following control of an AUV, *Ocean Eng.*, 34(2007) 1734-1744.
23 Xiang, X.B., Lapierre, L. & Jouvencel, B., Smooth transition of AUV motion control: From fully-actuated to under-actuated configuration, *Robot. Auton. Syst.*, 67(2015) 14-22.
24 Xiang, X.B., Yu, C.Y., Zhang, Q. & Xu, G.H., Path-following control for an AUV: Fully actuated versus under-actuated configuration, *Mar. Technol. Soc. J.*, 50(2016) 34-47.
25 Fossen, T.I. & Lekkas, A.M., Direct and indirect adaptive integral line-of-sight path-following controllers for marine craft exposed to ocean currents, *Int. J. Adapt. Control Signal Process.*, 31(2017) 445-463.
26 Mei, J.H. & Arshad, M.R., A hybrid artificial potential field method for autonomous surface vessel path planning in dynamic riverine environment, *Indian J. Mar. Sci.*, 44(2015) 1980-1994.
27 Peng, Z.H., Wang, J. & Wang, D., Distributed containment maneuvering of multiple marine vessels via neurodynamics-based output feedback, *IEEE Trans. Ind. Electron.*, 64(2017) 3831-3839.
28 Zheng, Z.W, Huang, Y.T., Xie, L.H. & Zhu, B., Adaptive trajectory tracking control of a fully actuated surface vessel with asymmetrically constrained input and output, *IEEE Trans. Control Syst. Technol.* (in press), 2017, DOI: 10.1109/TCST.2017.2728518.
29 Wang, N., Su, S.F., Yin, J.C., Zheng, Z.J. & Er, M.J., Global asymptotic model-free trajectory-independent tracking control of an uncertain marine vehicle: An adaptive universe-based fuzzy control approach, *IEEE Trans. Fuzzy Syst.* (in press), 2017, DOI: 10.1109/TFUZZ.2017.2737405.
30 Peng, Z.H., Wang, J. & Wang, D., Containment maneuvering of marine surface vehicles with multiple parameterized paths via spatial–temporal decoupling, *IEEE/ASME Trans. Mechatron.*, 22(2017) 1026-1036.
31 Subudhi, B., Mukherjee, K. & Ghosh, S., A static output feedback control design for path following of autonomous underwater vehicle in vertical plane, *Ocean Eng.*, 63(2013) 72–76.
32 Naik, M.S. & Singh, S.N., State-dependent Riccati equation-based robust dive plane control of AUV with control constraints, *Ocean Eng.*, 34(2007) 1711-1723.
33 Khodayari, M.H. & Balochian, S., Modeling and control of autonomous underwater vehicle (AUV) in heading and depth attitude via self-adaptive fuzzy PID controller, *J. Mar. Sci. Technol.*, 20(2015) 559-578.
34 Ishaque, K., Abdullah, S.S., Ayob, S.M. & Salam, Z., A simplified approach to design fuzzy logic controller for an underwater vehicle, *Ocean Eng.*, 38(2011) 271-284.
35 Yu, C.Y., Xiang, X.B, Zhang, Q. & Xu, G.H., Adaptive fuzzy trajectory tracking control of an under-actuated autonomous underwater vehicle subject to actuator saturation, *Int. J. Fuzzy Syst.* (in press), 2017, DOI: 10.1007/s40815-017-0396-9.
36 Miao, J.M., Wang, S.P., Zhao, Z.P., Li, Y. & Tomovic, M.M., Spatial curvilinear path following control of underactuated AUV with multiple uncertainties, *ISA Trans.*, 67(2017) 107-130.
37 Fredriksen, E. & Pettersen, K.Y., Global κ-exponential way-point maneuvering of ships: Theory and experiments, *Automatica*, 42(2006) 677-687.
38 Xiang, X.B., Yu, C.Y., Lapierre, L., Zhang, J.L. & Zhang, Q., Survey on fuzzy-logic-based guidance and control of marine surface vehicles and underwater vehicles, *Int. J. Fuzzy Syst.* (in press), 2017, DOI: 10.1007/s40815-017-0401-3.
39 Xiang, X.B., Yu, C.Y. & Zhang, Q., On intelligent risk analysis and critical decision of underwater robotic vehicle, *Ocean Eng.*, 140(2017) 453–465.
40 Ju, Z.J. & Liu, H.H., Fuzzy Gaussian mixture models. *Pattern Recogn.*, 45(2012) 1146–1158.
41 Yu, C.Y., Xiang, X.B., Lapierre, L. & Zhang, Q., Nonlinear guidance and fuzzy control for three-dimensional path following of an underactuated autonomous underwater vehicle, *Ocean Eng.*, 146(2017) 457–467.